Dalton Transactions

ROYAL SOCIETY OF CHEMISTRY

COMMUNICATION

View Article Online
View Journal | View Issue

Cite this: *Dalton Trans.*, 2020, **49**, 15171

Received 6th October 2020,
Accepted 23rd October 2020

DOI: 10.1039/d0dt03449e

rsc.li/dalton

Variable dimensionality in 'hollow' hybrid tin iodide perovskites†

Jason A. McNulty, Alexandra M. Z. Slawin and Philip Lightfoot *

Two 'hollow' B-site deficient perovskites, $(TzH)_{11}(H_3PO_2)Sn_6I_{23}$ and $(TzH)_3Sn_2I_7$ (TzH^+ = 1,2,4-triazolium, H_3PO_2 = hypophosphorous acid), have been prepared. $(TzH)_{11}(H_3PO_2)Sn_6I_{23}$ is the first example of a 2D layered structure of this type. Leaving the same reaction mixture for an extended time also affords the 3D derivative $(TzH)_3Sn_2I_7$.

Studies investigating dimensional reduction in organic–inorganic hybrid perovskite materials, from the 3D ABX_3 structure (A = organic or inorganic monovalent cation, B = Pb^{2+} or Sn^{2+}, X = Cl, Br or I), have become prevalent in recent years in an effort to obtain new materials with tuneable properties.[1–3] Many of these materials have generated interest due to their potential use in solar cells and light-emitting devices (LEDs) among others.[4,5] These studies have primarily focused on lead halide materials as these have been found to give the highest-efficiency perovskite solar cells thus far.[6,7]

However, these materials remain problematic due to the high toxicity of Pb and, as such, investigations into alternatives are becoming commonplace.[8] The most common examples replace Pb^{2+} with Sn^{2+} due to the similar electronic and optical properties that can be achieved in these perovskites.[9,10] In our previous work,[11] we presented two unusual examples of perovskite materials incorporating Sn, namely the 3D $(GuH)_{0.5}(TzH)_{0.5}SnI_3$ and 2D $(GuH)_{1.5}(Me\text{-}ImH)_{0.5}SnI_4$ (GuH^+ = guanidinium, TzH^+ = 1,2,4-triazolium and $Me\text{-}ImH^+$ = 1-methylimidazolium). Both of these materials featured unprecedented ordering patterns of organic cations, suggesting that further study of tin iodide-based perovskites could result in a diverse range of structure-types that have not been observed in hybrid perovskite materials thus far.

In this paper we present two new hybrid Sn iodide perovskite structures inspired by our previous work using TzH^+ as a structure-directing agent, which has previously led to the discovery of a wide variety of structural novelty.[11–13] Our nominal target composition was $(TzH)SnI_3$, which we assumed might adopt a 3D structure related to that observed in $(GuH)_{0.5}(TzH)_{0.5}SnI_3$. To our surprise the reaction produced a novel structure type based on a 'hollow' B-site deficient perovskite, $(TzH)_{11}(H_3PO_2)Sn_6I_{23}$ (**1**). While the B-site deficient perovskite structure has been reported previously,[14,15] **1** represents the first example of a layered variant of this family. On leaving the same reaction mixture for 2 months, a 3D 'hollow' perovskite $(TzH)_3Sn_2I_7$ (**2**) is the dominant product.

Details of the synthesis and characterisation are provided in the ESI.† In brief, the same reaction mixture produces **1** after ~1 h and **2** after ~2 months. The crystal structures of **1** and **2** were determined by single crystal X-ray diffraction at 93 K and 173 K, respectively: crystallographic details given in Table 1. While the amine and coordinated solvent, H_3PO_2, positions in **1** have been identified fully, it has not been possible to fully assign the C/N positions of TzH^+ as partial disorder precludes definitive atom assignment. In **2**, only the tin iodide framework has been included in the final refinement; the level of disorder is higher and although fragments can be assigned, no satisfactory and complete model of the amine moieties was found. Nevertheless, CHN analysis supports the proposed composition, with three intact TzH^+ moieties, hence we conclude there is no degradation of the amine during the prolonged reaction. Fig. 1 shows the crystal structures of **1** and **2** highlighting the B-site deficiency common to both compositions and the difference in connectivity between the 2D layered and 3D structures. For clarity, amine positions have been omitted. A key distinction between the two structures is the incorporation of a neutral H_3PO_2 molecule in **1**, which acts to 'cap' and separate the triple perovskite-like blocks.

In our previous work[11,13] we discussed the significant effect that ionic size, lone-pair effects and hydrogen-bonding environments can have on both cationic ordering behaviour and sub-

School of Chemistry and EaStChem, University of St Andrews, St Andrews, Fife, KY16 9ST, UK. E-mail: pl@st-andrews.ac.uk

†Electronic supplementary information (ESI) available: Synthesis, single crystal X-ray diffraction, crystallographic data (CIF). CCDC 2026398 (**1**) and 2026399 (**2**). For ESI and crystallographic data in CIF or other electronic format see DOI: 10.1039/d0dt03449e

Table 1 Crystallographic data and refinement details for **1** and **2**

	1	**2**
Temperature	93 K	173 K
Formula[a]	$C_{22}N_{33}H_{47}PO_2Sn_6I_{23}$	$C_6N_9H_{12}Sn_2I_7$
Formula weight	4423.95	1335.97
Density/g cm^{-3}	3.220	2.801
Crystal system	Triclinic	Triclinic
Space group	$P\bar{1}$	$P\bar{1}$
a/Å	14.0051(14)	6.403(4)
b/Å	14.7298(13)	14.2301(10)
c/Å	22.5350(20)	14.680(11)
α/°	83.978(5)	91.42(3)
β/°	85.573(5)	93.54(3)
γ/°	88.147(6)	90.10(3)
V/Å^3	4608.0(7)	1334.6(13)
Z	2	2
Measured ref.	130 747	36 319
Independent ref.	16 815 [R(int) = 0.0869]	4844 [R(int) = 0.1379]
Refined parameters	794	85
GOOF	1.128	1.837
Final R indices ($I > 2\sigma(I)$)	R_1 = 0.0593, wR_2 = 0.1381	R_1 = 0.1758, wR_2 = 0.4900

[a] C/N positions in **1** have not been fully assigned as disorder precludes definitive atom assignment. While only the tin iodide framework of **2** has been refined, the formula and formula weight has been calculated based on the assumed $(TzH)_3Sn_2I_7$ composition.

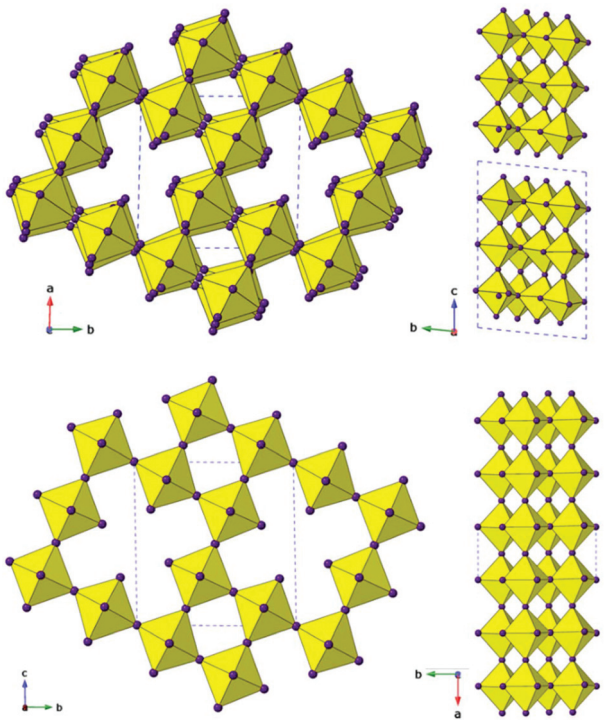

Fig. 1 Inorganic framework of **1** (top) at 93 K and **2** (bottom) at 173 K. Note the B-site deficiency common to both **1** and **2** (left) and the difference in connectivity (right) between the layered 2D and 3D structure-types observed in **1** and **2**, respectively. Note that the 'triple' perovskite-like blocks in **1** are partially staggered relative to each other along c (see Fig. 2d).

sequent structural distortions in tin iodide perovskites. In **1**, there are several amine environments of importance and these are shown in Fig. 2. Previously we discussed the lack of octahedral tilting in $(GuH)_{0.5}(TzH)_{0.5}SnI_3$ and the occurrence of considerable octahedral distortions. While it might reasonably be assumed that a similar distortion would be present in the 'perovskite unit' of the network in **1** this is not the case. Instead conventional tilting of the octahedra occurs to optimise bonding and accommodate the TzH^+ cation, as shown in Fig. 2a. The accommodation of a TzH^+ cation in the 'hollow' at the vacant B-site leads to an unusual coordination environment, as shown in Fig. 2b. In this environment the central TzH^+ cation forms inter-amine hydrogen-bonds to two other TzH^+ cations. Due to the space requirements of the N lone-pair, both of the remaining TzH^+ orient with this pointing towards the central cation. This results in an interaction reminiscent of lone pair-π stacking (Fig. 2c).[16,17] While this type of interaction is weak, it would be expected to have a slight stabilising effect on the structure. Perhaps the most interesting amine environment in **1** is that observed in the interlayer region. TzH^+ cations and H_3PO_2 molecules are arranged in a bilayer with each H_3PO_2 coordinated to two TzH^+ cations (only one of which is from the same layer). These are held by strong hydrogen bonds (N–H···O ~2.6–2.8 Å), likely contributing to the stability of this unique layered B-site deficient structure. In Fig. 2e the coordination of (H_3PO_2) to TzH^+ cations is shown. This highlights the presence of partial disorder within TzH^+ that precludes full assignment of C/N positions.

The mean distortion level (Δd) and bond angle variance (σ^2) of each octahedron in both compositions were calculated (details are provided in ESI†) and the values shown in Table 2. It can be noted that the most extreme octahedral distortions in **1** occur for Sn4 and Sn5, which are the two sites in the 'inner' layer of the triple perovskite block. Comparison of the structural distortions of **1** and **2** to previously reported materials is important in attempting to understand the adoption of the 2D and 3D structure-types, respectively. While at present there are five examples of 'hollow' B-site deficient tin iodide perovskites based on the $FASnI_3$ or $MASnI_3$ framework (FA^+ = formamidinium and MA^+ = methylammonium),[14,18,20,21] the crystal structure of the tin iodide framework of only one of these has thus far been determined, namely $HEA_xFA_{1-x}Sn_{0.67}I_{2.33}$ (HEA^+ = hydroxyethylammonium).[18] **1** is the first of these structure-types to include resolved amine positions. The mean distortion level in both **1** and **2** is greater than in either $HEA_xFA_{1-x}Sn_{0.67}I_{2.33}$ or the related Pb-based composition, $MA_{0.55}HEA_{0.63}Pb_{0.63}I_{2.82}$. While a greater distortion is expected in Sn-based structures compared to related Pb-based materials the magnitude of the difference does not solely account for this. We hypothesise that the presence of only a single small amine, TzH^+, in both **1** and **2** likely results in a greater distortion of the octahedra to optimise the hydrogen-bonding environments and stabilise the structure. This is in contrast to the linear HEA^+ present in both known materials which apparently somewhat precludes this distortion.

In summary, we have prepared two new examples of 'hollow' B-site deficient tin halide perovskites. In $(TzH)_{11}(H_3PO_2)Sn_6I_{23}$ we introduce the first 2D layered structure of this type and the first crystal structure featuring resolved amine positions. In

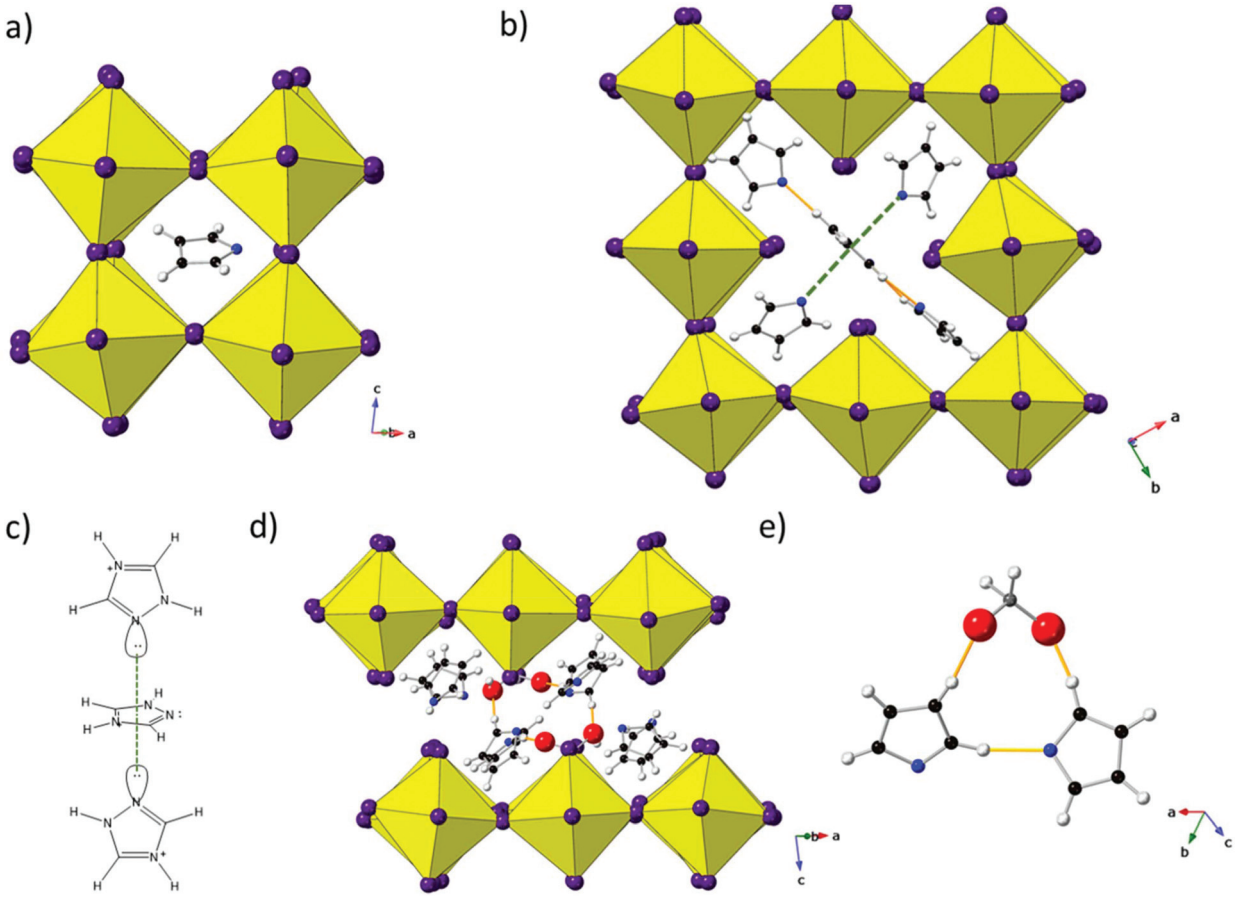

Fig. 2 Different amine environments in **1**. (a) Octahedral tilting in the 'perovskite unit'; (b) 'hollow' B-site deficient coordination of TzH^+ showing inter-amine hydrogen-bonding and lone pair-π stacking-like interaction; (c) schematic of the lone pair-π stacking interaction; (d) interlayer TzH^+ interaction with (H_3PO_2); (e) strong hydrogen-bonding of TzH^+ to (H_3PO_2). Hydrogen-bonding and the lone-pair-π stacking-like interaction are shown by the solid orange and dashed green lines, respectively.

Table 2 Summary of calculated bond length distortions (Δd) and bond angle variance (σ^2) for B-site deficient compounds reported here and in the literature

Composition	B cation	Δd ($\times 10^{-4}$)	σ^2
1	Sn1	27.00	14.37
	Sn2	19.77	7.32
	Sn3	18.48	12.92
	Sn4	46.79	24.77
	Sn5	32.56	30.54
	Sn6	21.86	8.73
2	Sn1	30.52	7.62
	Sn2	18.92	7.90
$HEA_xFA_{1-x}Sn_{0.67}I_{2.33}$ [18]	Sn1	17.47	1.43
$MA_{0.55}HEA_{0.63}Pb_{0.63}I_{2.82}$ [19]	Pb1	5.88	4.98

$(TzH)_3Sn_2I_7$ we present the first structure of this type templated by a single organic cation. The occurrence of two distinct compounds in this reaction sequence may be due to a structural change from **1** to **2** over time, but other processes such as the delayed precipitation of **2** or the initial presence of both **1** and **2** simultaneously followed by dissolution of **1** cannot be ruled out. **2** represents the first 3D 'hollow' perovskite templated using a single cation. The versatility of 1,2,4-triazolium as a structure-directing agent in hybrid perovskites has resulted in the discovery of several previously unseen structures that likely would not have been realised otherwise. Moreover, the first observation of the inclusion of H_3PO_2 as an active 'capping' agent provides food-for-thought in the design of dimensionally-reduced perovskites. This work prompts further study of the structure-directing effects of both small disc-shaped amines and hypophosphorous acid in the pursuit of interesting new structure-types, ultimately with prospects for property manipulation and control.

Conflicts of interest

There are no conflicts to declare.

Acknowledgements

We acknowledge support from the University of St Andrews and the Leverhulme trust (RPG-2018-065). The research data

supporting this publication can be accessed at 10.17630/30969c0d-61c9-4f69-822b-f953ae580ec7.

Notes and references

1 B. Saparov and D. B. Mitzi, *Chem. Rev.*, 2016, **116**, 4558–4596.
2 M. D. Smith, B. A. Connor and H. I. Karunadasa, *Chem. Rev.*, 2019, **119**, 3104–3139.
3 G. Grancini and M. K. Nazeeruddin, *Nat. Rev. Mater.*, 2019, **4**, 4–22.
4 L. Mao, W. Ke, L. Pedesseau, Y. Wu, C. Katan, J. Even, M. R. Wasielewski, C. C. Stoumpos and M. G. Kanatzidis, *J. Am. Chem. Soc.*, 2018, **140**, 3775–3783.
5 X. Li, J. Hoffman, W. Ke, M. Chen, H. Tsai, W. Nie, A. D. Mohite, M. Kepenekian, C. Katan, J. Even, M. R. Wasielewski, C. C. Stoumpos and M. G. Kanatzidis, *J. Am. Chem. Soc.*, 2018, **140**, 12226–12238.
6 J. Li, H. Wang, X. Y. Chin, H. A. Dewi, K. Vergeer, T. W. Goh, J. W. M. Lim, J. H. Lew, K. P. Loh, C. Soci, T. C. Sum, H. J. Bolink, N. Mathews, S. Mhaisalkar and A. Bruno, *Joule*, 2020, **4**, 1035–1053.
7 C. Lin, *Front. Chem.*, 2020, **8**, 592.
8 Z. Xiao, Z. Song and Y. Yan, *Adv. Mater.*, 2019, **31**, 1803792.
9 C. C. Stoumpos, C. D. Malliakas and M. G. Kanatzidis, *Inorg. Chem.*, 2013, **52**, 9019–9038.
10 W. Ke, C. C. Stoumpos and M. G. Kanatzidis, *Adv. Mater.*, 2019, **31**, 1803230.
11 J. A. McNulty and P. Lightfoot, *Chem. Commun.*, 2020, **56**, 4543–4546.
12 Y. Guo, L. Yang, S. Biberger, J. A. McNulty, T. Li, K. Schötz, F. Panzer and P. Lightfoot, *Inorg. Chem.*, 2020, **59**, 12858–12866.
13 Y.-Y. Guo, J. A. McNulty, N. A. Mica, I. D. W. Samuel, A. M. Z. Slawin, M. Buhl and P. Lightfoot, *Chem. Commun.*, 2019, **55**, 9935–9938.
14 W. Ke, C. C. Stoumpos, M. Zhu, L. Mao, I. Spanopoulos, J. Liu, O. Y. Kontsevoi, M. Chen, D. Sarma, Y. Zhang, M. R. Wasielewski and M. G. Kanatzidis, *Sci. Adv.*, 2017, **3**, 1–10.
15 W. Gao, C. Chen, C. Ran, H. Zheng, H. Dong, Y. Xia, Y. Chen and W. Huang, *Adv. Funct. Mater.*, 2020, **1**, 1–29.
16 T. J. Mooibroek, P. Gamez and J. Reedijk, *CrystEngComm*, 2008, **10**, 1501–1515.
17 J. Novotný, S. Bazzi, R. Marek and J. Kozelka, *Phys. Chem. Chem. Phys.*, 2016, **18**, 19472–19481.
18 C. M. Tsai, Y. P. Lin, M. K. Pola, S. Narra, E. Jokar, Y. W. Yang and E. W. G. Diau, *ACS Energy Lett.*, 2018, **3**, 2077–2085.
19 A. Leblanc, N. Mercier, M. Allain, J. Dittmer, V. Fernandez and T. Pauporté, *Angew. Chem., Int. Ed.*, 2017, **56**, 16067–16072.
20 W. Ke, C. C. Stoumpos, I. Spanopoulos, M. Chen, M. R. Wasielewski and M. G. Kanatzidis, *ACS Energy Lett.*, 2018, **3**, 1470–1476.
21 W. Ke, C. C. Stoumpos, I. Spanopoulos, L. Mao, M. Chen, M. R. Wasielewski and M. G. Kanatzidis, *J. Am. Chem. Soc.*, 2017, **139**, 14800–14806.